Chapter 3

To identify the novel GCase chaperones for Parkinson's disease treatment: *In silico* screening and *in vitro* investigation

3 Introduction

Glucocerebrosidase (GCase, EC: 3.2.1.45) is a lysosomal acid glycoside hydrolase (GH) that belongs to family 30 and is encoded by the GBA1 gene (Mazzulli, Zunke et al. 2016). The GBA1 gene is one of the genes linked to lysosomal storage disorders (LSDs), which account for 56% of instances of Parkinson's disease (PD) (Robak, Jansen et al. 2017). The disease-modifying therapy for PD with dementia is currently being developed with GCase chaperone (Ambroxol, AMB) (ClinicalTrials.gov Identifier, NCT02914366) (Silveira, MacKinley et al. 2019). Sub-chronic treatment of AMB has a disease-modifying effect through increasing GCase activity in 6-hydroxydopamine hydrochloride (6-OHDA, neurotoxic) induced rat PD model (Mishra and Krishnamurthy 2020). AMB's neuroprotective effects have already been documented (Bhardwaj, Arunachalam et al. 2016). However, all these effects were only seen at higher doses of AMB (800-1000 mg/kg *p.o*) due to issues with BBB. There are currently no licensed drugs available for neuroprotection or neurorestoration treatment for PD in people with GCase deficiency, despite the fact that GCase has a potential role in PD pathogenesis. Hence, there is a need to discover novel potential GCase chaperones with disease-modifying potential for the treatment of PD.

Decreased GCase activity has been observed in several brain regions of both PD patients and rat models of the disease (Gegg, Burke et al. 2012, Rocha, Smith et al. 2015, Mishra, Chandravanshi et al. 2018). However, here we cannot overlook the reality that rats are a widely used animal model employed in drug discovery to screen anti-PD molecules (Blandini, Armentero et al. 2008). Hence, in this study, we have chosen rat glucocerebrosidase (rGCase) homology modeling to screen novel hits as anti-PD molecules against rGCase. The details of rGCase homology modeling and validation have

been described earlier (Tripathi, Ganeshpurkar et al. 2022). A fully folded GCase constitutes 515 amino acid residues, three domains, and a molecular weight of 60 kDa. Domain I contains Ala20 – Asp46 and Leu401 – Gln432 and is tightly joined with domain III (residues Gnl95 – Trp399 and Met434 – Gly448). Domain II (residues Thr49 – Phe94 and Ser450 – Gln515), on the other hand, appears to be linked by a pliable hinge to domain III, which contains the GCase active site cavity. This cavity is surrounded by residues Arg139, Asp146, Phe147, Trp198, Asn253, Glu254, Ala257, Tyr263, Phe265, Gln266, Cys267, Tyr331, Met332, Asp33, Phe334, Leu335, Ala336, Glu358, Cys360, Ser363, Lys364, Phe365, Trp399, Asp414, Phe415, and Val416. Also, a few loops (loop 1; His329 – Pro337, loop 2; Cys360 – Leu373, loop 3; Val412 – Asp417, loop 4; Ser256 – Cys267) have been present at the entrance of the cavity in such a way that they hold the ligand inside the cavity. The configurations or orientations of these loops are extremely pH sensitive and supple. Due to this, they change their configuration at a divergent pH medium while trafficking GCase from the ER (neural pH: 7.0) to lysosomes (acidic pH 5.0-4.5) (Smith, Mullin et al. 2017, Jana, Ganeshpurkar et al. 2018, Tripathi, Ganeshpurkar et al. 2022).

Chaperones are identified as potential therapeutic agents for disease-modifying therapy of PD due to their GCase stabilizing activity (Silveira, MacKinley et al. 2019). Unfortunately, AMB is the only GCase chaperone that is entered into the clinical trial as a disease-modifying agent for PD. However, its capacity to penetrate the CNS is still up for debate (Weiser and therapeutics 2008, Silveira, MacKinley et al. 2019). To our knowledge, no approved GCase chaperones are currently available that have GCase stabilizing action as well as disease-modifying effects in PD. The process to select

suitable chaperones with more protein stabilising potential through virtual screening during the drug discovery process is still unexplored.

Our main goal is to employ computational drug discovery techniques to find new possible GCase chaperones based on the AMB scaffold with the disease-modifying potential to treat PD. By using *in silico* pH-dependent molecular docking and molecular dynamics simulation; the capacity of screened compounds to stabilize GCase was assessed, and its effectiveness was then verified *in vitro* (pH-dependent binding affinity, enzyme inhibition mechanism, and structural stability assay). Finally, to validate the stability of the protein-ligand complex, the most promising molecule was investigated by circular dichroism (CD), FT-IR, and Raman spectroscopy. To examine their potential as GCase chaperones for the treatment of PD, cell lines were used. **Figure 3.1** provides a comprehensive visualization of the screening and evaluation process employed in the GCase chaperoning assay. This workflow diagram effectively portrays the key steps involved in the systematic assessment of compounds.

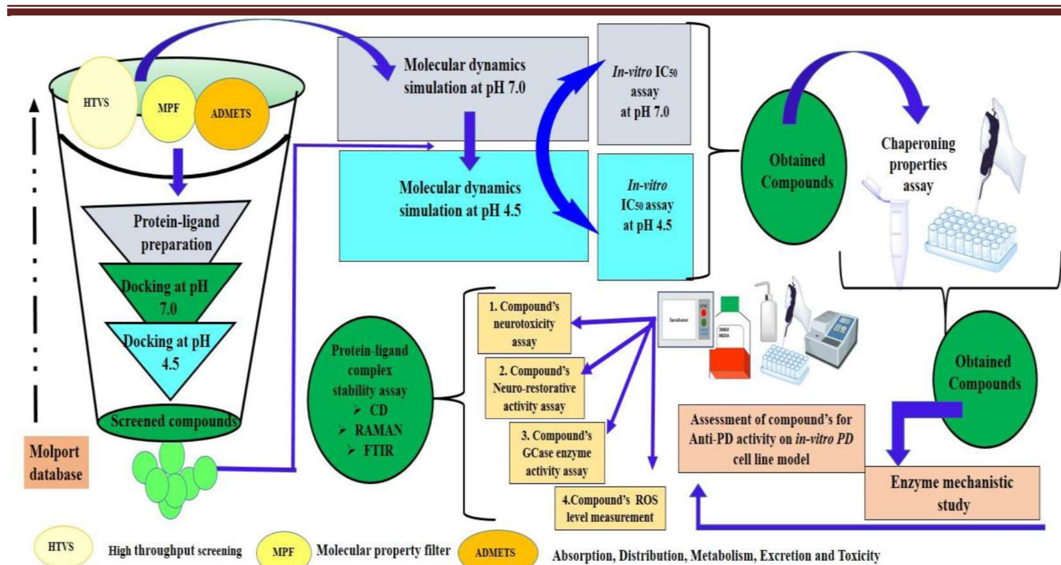

Figure 3.1 Schematic work flow of the objective 3

3.1 Material and method

3.1.1 Reagents

SH-SY5Y (neuroblastoma) cell line was acquired from the Pune National Centre of Cell Science (NCCS). DMEM/F12 procured from Gibco Life Technologies, USA. Heat-inactivated fetal bovine serum (FBS) and 2'7'-dichlorofluorescein diacetate (DCF-DA) was procured from Thermo fisher. The top screened compounds (Code, MolPort-029-998-466: GC466, MolPort-029-998-519: GC519, MolPort-002-157-329: GC329 and MolPort-002-153-607: GC607) were procured from the Mole-port database. 6-OHDA was procured from Cayman chemicals. All other reagents used were of analytical grade.

3.1.2 Homology modeling and validation

rGCase homology modeling was constructed and validated at pH 7.0 and 4.5 according to our previously published protocol (Ganeshpurkar, Kumar et al. 2018, Tripathi, Ganeshpurkar et al. 2022).

3.1.3 *In silico* study

3.1.3.1 High-throughput virtual screening based on pharmacophore, PAINS, molecular, and ADMET property filters

The tanimoto similarity index webserver was used for screening AMB-like scaffolds from the Molport database. The molecular property of the obtained molecules was calculated through PAINS (pan assay interference compounds) followed by Biosigs's pkCSM web server (http://biosig.unimelb.edu.au/pkcsm/prediction) using SMILES strings of the compounds (Ganeshpurkar, Singh et al. 2022, Tripathi, Ganeshpurkar et al. 2022).

3.1.3.2 Virtual molecular docking

Chem3D was used to convert the ligands SMILES input to three-dimensional structures. The ligands' energies were minimized using MMFF94's force field and saved as PDB files. Autodock Tools-1.5.6 was used to convert PBD into PDBQT files. The grid was mapped by the Autogrid 4.0 tool to ensure the envelopment of the active site region. The parameters for the grid were fixed at grid box size: 54×62×74; grid spacing: 0.375 Å; and grid center for x*,* y*, and* z, coordinates 11.177, -7.564, and 38.121, respectively. Autodock 4.2 was used for the virtual docking of obtained hits. The docked structure was examined by Discovery studio visualizer 2021 (Ganeshpurkar, Singh et al. 2022, Tripathi, Ganeshpurkar et al. 2022)

3.1.3.3 Molecular dynamics (MD) simulation

Desmond v2.2, Schrodinger 2015-1 tool was used to run the MD of protein, protein-ligand complexes, and specific ligands. Chapter I describes the specifics of MD simulation and their parameters (Ganeshpurkar, Singh et al. 2020, Singh, Ganeshpurkar et al. 2020, Ganeshpurkar, Singh et al. 2022, Tripathi, Ganeshpurkar et al. 2022).

3.1.4 *In vitro* pH-dependent enzyme mechanistic study

3.1.4.1 Estimation of IC_{50}

We employed seven concentrations of test substances (0-1000 μM) and evaluated them on rGCase at pH 7.0 and 4.5 of McIlvaine buffer (100 mM citric acid, 200 mM sodium phosphate buffer) to determine IC_{50} values, as detailed in our earlier study (Tripathi, Ganeshpurkar et al. 2022). Fluorescence was taken in Synergy HTX multi-mode reader (BioTek, USA) at ex: em; 355:460 nm wavelength. The plots of log inhibitor concentrations (log [I]) against % fluorescence signals were used to extract IC_{50} values. The experiment was repeated three times, and the results are mentioned in means ± standard deviations (Graph Pad Prism 5.1 Software, Inc.).

3.1.4.2 Evaluation of test compounds chaperoning property

The potential chaperoning properties of the test compounds were determined by studying rGCase stability after heat exposure. The reactions were carried out in two sets of identical plates, each containing 50 µl of rGCase fractions (20 µg / µl) and various concentrations (**concentrations mentioned in Table 3.3**) of test compounds. One plate was kept on ice, while the other was incubated at 48 °C for over 60 minutes to denature the rGCase and then returned to room temperature for 10 min for equilibration. Later, 100 μl of the substrate 4-MUG (4 Mm, final concentration), and incubated further for 15 min at 37 °C. The fluorescence was recorded after quenching the enzyme reaction with Glycine buffer (pH=10.6). Relative enzyme activity (RA) and stabilization ratio (SR) after thermal denaturation were recorded using the following formula in triplicate for each experiment (Trapero, Gonzalez-Bulnes et al. 2012, Tripathi, Ganeshpurkar et al. 2022).

$$\textbf{\textit{Eqation}}\ \mathbf{1} \qquad RA = \left[\frac{\text{Fluorescence units measured in each well incubated at 48 °C}}{\text{Fluorescence units in the corresponding well kept at 0 °C}}\right]$$

$$\textbf{\textit{Equation}}\ \mathbf{2} \qquad SR = \left[\frac{\text{Relative enzyme activity in presence of test compounds}}{\text{Relative enzyme activity in the corresponding time of controls}}\right]$$

3.1.4.3 Binding mode Study

A reversibility study was conducted to investigate the enzyme's binding mode at pH 7.0. Test compounds were incubated with 10 µg (0.5 µg of protein/µl) of rGCase at concentrations of 10 × IC_{50} and 100 × IC_{50} for 30 minutes on ice. Subsequently, the samples were diluted 100-fold with its substrate (4-MUG, 2.5 mM final concentration, freshly prepared in McIlvaine buffer) to achieve final inhibitor concentrations of 0.1 × IC_{50} and 1 × IC_{50}, respectively. Fluorescence measurements were taken at ex: em; 355:460 nm. The negative control (without test compounds) was interpreted as 100 % enzyme activity. The residual enzyme activity in triplicates after dilutions were measured and expressed as mean ± SD (Minders, Petzer et al. 2015, Kumar, Dwivedi et al. 2018).

3.1.4.4 Enzyme kinetics

An enzyme kinetics assay was conducted to gain deeper insights into the mechanism of enzyme action for the test compounds at a pH of ER (7.0), where the test compounds exclusively bind. In order to study enzyme kinetics, different concentrations of the substrate and test compounds (**as indicated in Figure 3.10**) were employed. Each concentration of tests was incubated with various concentrations of substrate. Compound concentrations of 0.5 X IC_{50}, 1 X IC_{50}, and 2 X IC_{50} of pH 7.0 IC_{50} were used. For 10 minutes, the fluorescence was measured every 2 minutes. Graph Pad Prism 5.1 was used

to calculate the Michaelis-Menten constant (K_m) and maximum reaction rate (V_{max}) values; however, the Dixon plot was used to extract K_i (X-axis intercept). All assay datasets were presented as a mean ± SD (Gutti, Kumar et al. 2019, Tripathi, Ganeshpurkar et al. 2022).

3.1.5 Cell line studies

SH-SY5Y, a neuroblastoma cell line, was used for this study as it has been widely used for PD research. Cells were grown at 37 ^{0}C in a DMEM/F12 medium supplemented with 10% heat-inactivated fetal bovine serum, 50 U/ml penicillin, 100 µg/ml streptomycin and 10 µM all-trans-retinoic acid in an incubator under humidified condition (5% CO2/95% air) (Ahmad, Fatima et al. 2021).

3.1.5.1 Neurotoxicity assay

The test compounds' neurotoxicity was measured in terms of cell viability by MTT (3-(4,5-dimethylthiazol-2-yl)-2,5-diphenyltetrazolium bromide) assay in accordance with the previously described protocol with some modifications (Venuprasad, Hemanth Kumar et al. 2013, Wang, Liu et al. 2017, Ahmad, Fatima et al. 2021). Briefly, cells were seeded overnight in 96-well plates at a density of 5.0×10^3 cells per well before experimentation. The next day, media were replaced with fresh media containing a graded concentration (mentioned in **Figure 3.11**) of test compounds and incubated for 48 hours (hr) at 37 °C. Each compound was dissolved in DMSO, and the media's total DMSO content was less than 1%, with no toxic effect on cell viability. Next, the medium in each well was aspirated, replaced with a fresh medium containing 5 mg/ml MTT, and further incubated for 4 hr at 37 °C. MTT solution was removed from each well; the remaining MTT formazon crystals were dissolved in 250 µl DMSO. The absorbance was measured

by a microplate reader at 550 nm. Values were taken in triplicate and expressed as a % of the control in the form of mean ± SD.

3.1.5.2 Evaluation of test compounds on 6-OHDA-induced PD cell line model

The experiment was followed in accordance with the protocol described in **section 3.1.7.2.** Briefly, cells were first exposed to 100 and 150 µM of 6-OHDA (freshly prepared in 0.02 % ascorbic acid) for 0 - 24 hrs to determine the time taken to develop PD in terms of neurotoxicity (Venuprasad, Hemanth Kumar et al. 2013, Wang, Liu et al. 2017, Ahmad, Fatima et al. 2021).

3.1.5.3 Neurorestorative activity assay

Cells were pre-exposed with 150 µM of 6-OHDA for 6 hr before being exposed to various concentrations (mentioned in **Figure 3.12**) of test compounds for 48 hr to determine the neurorestorative effect of test compounds. The time and concentration of 6-OHDA were chosen based on our **section 3.1.7.2** experiment. The response was calculated as a % of the control, represented as mean ± SD (Venuprasad, Hemanth Kumar et al. 2013, Ahmad, Fatima et al. 2021).

3.1.5.4 GCase activity assay

The GCase assay was performed according to the previously established method with slight modifications (Trapero, Gonzalez-Bulnes et al. 2012). Initially, 5.0×103 cells were seeded onto the wells and allowed to adhere overnight in a CO2 incubator with a 5% CO2 atmosphere. After the predetermined treatment and incubation duration of the test compounds with 6-OHDA **(as outlined in section 3.1.7.2)**, the media from each well was carefully removed. Subsequently, to this 50 µl of PBS and 50 ul of McIlvaine buffer (100 mM citric acid, 200 mM sodium phosphate buffer, pH 4.5) were added. To initiate the

enzymatic reactions, 100 µL of 5 mM of 4-MUG was added to each well and incubated for 2 hr at 37 °C. By lysing the cells in 1.8 mL of glycine/ NaOH buffer (100 mM, pH 10.6), enzymatic reactions were halted, and liberated 4-MU was measured (ex: em; 355:460 nm). All values are shown as mean ± SD and repeated three times (Graph Pad Prism 5.1 Software, Inc.)

3.1.5.5 Measurement of Reactive oxygen species (ROS) level

The level of intracellular reactive oxygen species (ROS) was assessed using 2',7'-dichlorofluorescein diacetate (DCF-DA). DCF-DA is a nonfluorescent dye that is sensitive to oxidative changes. Upon entry into the cells, DCF-DA is subjected to oxidation by intracellular ROS, leading to the formation of a fluorescent compound known as 2',7'-dichlorofluorescein (DCF). The intensity of fluorescence emitted by DCF was utilized as an indicator of the overall generation of ROS within the cells, as previously described (Guo, Bezard et al. 2005). Following the prescribed treatment and incubation period for 6-OHDA with test compounds (**detailed in section 3.1.7.2**), cells were washed and incubated with 10 µM DCF-DA for 30 min in the dark. Quantification was performed using a fluorescence microplate reader at ex: em (490 nm: 520 nm) wavelength and expressed as normalized fluorescence intensity (NFI) relative to control wells.

3.1.5.6 Measurement of protein-ligand interaction stability

The conformational changes in rGCase and stability of protein-ligand interactions affected by pHs were further validated by CD, FT-IR, and Raman spectroscopies in line with a method that has previously been reported with a few modifications (Xu, Han et al. 2011, Bi, Tang et al. 2016, Han, Fang et al. 2017). The **appendices [Page 227 – 233]** comprehensively describes the protocol's characteristics. Each spectrum represents an average of three scans. Spectroscopic data were analyzed to identify secondary structures

such α-helix, β-sheet, and random coil using the BESTSEL web tool (https://bestsel.elte.hu/index.php). However, Origin software (version 6.0, Northampton, MA, USA) was used to analyses the FT-IR and Raman spectra.

3.2 Data and statistical analysis

GraphPad Prism 5.1 and Microsoft Excel version 20 were used to analyze all the experimental datasets and presented as mean ± SD. Statistical significance between two or more groups was analyzed by one-way ANOVA followed by Post-hoc Tuckey or Bonferroni multiple comparison tests using Graph Pad Prism 5.1. In the analysis of the aggregate datasets, $p < 0.05$ was considered significant.

3.3 Result and discussion

3.3.1 Homology modeling and validation

Ideally, chaperones are bound to GCase at the condition of ER pH (neutral, 7.0) and elute at lysosomal pH (acidic, pH 4.5) (Bendikov-Bar, Maor et al. 2013, Smith, Mullin et al. 2017). Thus, we built its homology modeling at both pHs. The details of the rGCase homology modeling, validation, and obtained active site residues are discussed in the chapter II and our previous study (Tripathi, Ganeshpurkar et al. 2022). The rGCase active site contains the amino acids Arg139, Asp146, Phe147, Trp198, Asn253, Glu254, Ala257, Tyr263, Phe265, Gln266, Cys267, Tyr 331, Met332, Asp333, Phe334, Leu335, Ala336, Glu358, Cys360, Ser363, Lys364, Phe365, Trp399, Asn414, Phe415, and Val416. In addition, four loops in and around the cavity have been identified, including loop 1; 329–337, loop 2; 360–373, loop 3; 412–417, and loop 4; 256–267, which aid in ligands recognition and grasping within their the cavity (**Figure. 3.1 in Appendices**].

3.3.2 High-throughput virtual screening based on pharmacophores, PAINS, molecular and ADMET property filter

The pharmacophore-based virtual screening was performed based on the Tanimoto similarity index, where similarity index ranges from 0 to 1 were chosen for selecting AMB-like scaffolds from the Molport database. We fixed the cutoff falling between 0.6 - 0.9. Higher values indicated greater similarity, while lower values indicated lower similarity. Obtained molecules passed through the PAINS filter, which was used to remove those molecules, may provide false results in high-throughput screening. Biosigs's pkCSM server was used to further filter the obtained compounds based on molecular and ADMET properties **(Table 3.1)**.

Table 3.1 The molecular properties and ADMET profiles of the best four ligands

Ligand ID[a]	**IUPAC name**	**MW[b]**	**LogP**	**THB[c]**	**RB[d]**	**BBB[e]**	**HIA[f]**	**hERG[g]**	**ROF[h]**	**CYP1A2/ CYP2C19/ CYP2C9/ CYP3A4 inhibitors**	**DL[i] / PAINS - FP[j]**	**Carcino _Mouse**	**Carcino _Rat**
MolPort-029-998-466	N-[(3-bromo-4-methoxyphenyl)methyl]cycloheptanamine hydrobromide	393.2	4.8	3	4	Yes	88.8	No	0	No	Yes	Negative	Negative
MolPort-029-	N-[(3-bromo-4-methoxyphenyl)methyl]cy	365.1	4.5	4	4	Yes	89.6	No	0	No	Yes	Negative	Negative

998-519	clopentanamine hydrobromide												
MolPort-002-157-329	N-[(3-bromo-4-methoxyphenyl)methyl]adamantan-1-amine	350.3	4.1	3	4	Yes	87.2	No	0	No	Yes	Negative	Negative
MolPort-002-153-607	N-[(2-bromophenyl)methyl]adamantan-2-amine	320.3	4.37	3	4	Yes	88.76	No	0	No	Yes	Negative	Negative

[a] Molport database compounds ID, [b] Molecular weight, [c] Total number of hydrogen bond, [d] No. of rotational bond, [e] Blood brain barrier penetrability, [f] Human intestinal absorption (% absorbed), [g] hERG: human ether-'α go-go related gene inhibitor, [h] Rule of five: No. of violations of Lipinski's rule of five (0 is good and 4 is bad), [i] Drug-likeness, and [j] Pan-assay interference compounds filter pass.

Molecular property filters considered parameters: molecular weight <450; logP <5; H-bond donor <3; H-bond acceptor <7; the number of rotatable bonds <8; and the total number of H-bonds <8. The limits of the above properties were determined after researching the physicochemical properties of CNS active compounds (Goldin, Zheng et al. 2012, Ganeshpurkar, Singh et al. 2020).

ADMET calculates the absorption, distribution, metabolism, excretion, and toxicity of the screened compounds. It is predicted that based on the percent of human intestinal absorption (HIA), a drug will be considered well absorbed if the HIA is greater than 70%. Numerous medications have been withdrawn from the market due to their ability to inhibit the human ether-'go-go-related gene (hERG), which frequently causes cardiac arrhythmia and sudden death (Singh, Ganeshpurkar et al. 2020). Furthermore, it is necessary to determine whether the screened compounds interact with the cytochromes P450 (CYP) isozyme superfamily (CYP1A2, CYP2C19, CYP2C9, CYP2D6, and CYP3A4), which are critical for drug elimination through metabolic biotransformation. These enzyme inhibitions lead to pharmacokinetics-related drug-drug interactions, resulting in toxic or other undesirable side effects due to decreased clearance and accumulation of the drugs. The other toxicity parameter is to test the carcinogenicity of obtained compounds using rodent carcinogenicity model. This model was created using toxicological data from rats and mice obtained from the National Toxicology Program and the US-FDA (Ganeshpurkar, Singh et al. 2020, Singh, Ganeshpurkar et al. 2020). As a result, 101 compounds in the current investigation were shown to have drug-like characteristics without deviating from any of the aforementioned standards.

3.3.3 *In silico* study

3.3.3.1 Virtual molecular docking

Virtual molecular docking was performed to gain insight into the binding mechanism of the ligands with the protein (Singh, Ganeshpurkar et al. 2020). Chaperones are pH-dependent enzyme inhibitors that bind to GCase with greater affinity at pH 7.0 but elute more easily from its active site cavity at pH 4.5 (Nakagome, Kato et al. 2018). Thus, we first selected pH 7.0 for virtual docking and assessed whether the 101 obtained hits interacted with rGCase at this pH. The results of pH 7.0 are shown in **Figure 3.2**, where we partitioned the docked hits based on BE to find the optimal BE ranges for hits that may act as chaperones. Next, based on BE, one best hit was selected from each BE range (four final hits) and docked them at pH 4.5. The BE and interaction patterns of pH 4.5 hits were compared with those of pH 7.0 hits to determine their pH-dependent interaction patterns (chaperoning behavior).

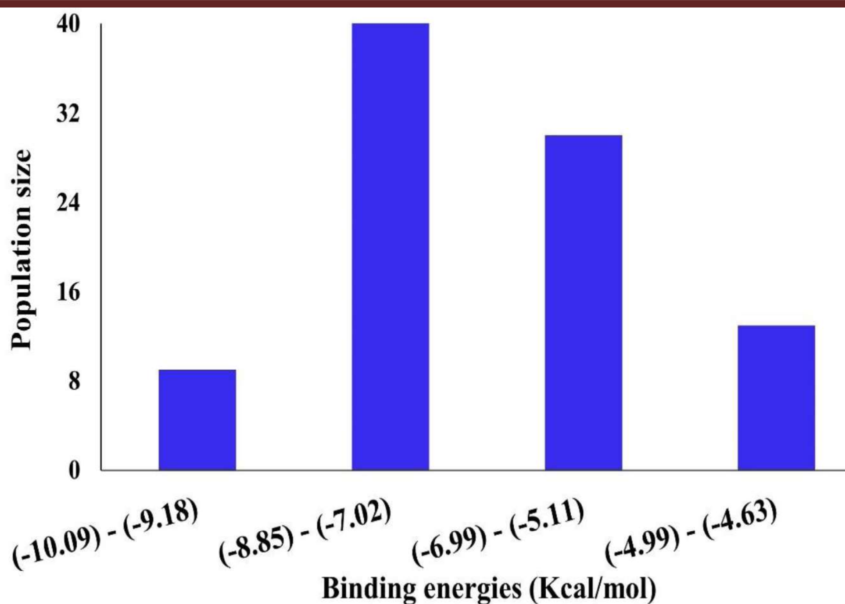

Figure 3.2 Distribution of docked hits based on binding energies at pH 7.0. Population size denotes the total number of compounds.

We found that among all compounds, GC466 and GC519 interacted with rGCase with the appropriate BE (GC466: -8.92 ± 0.68 Kcal/mol and GC519: -9.66 ± 1.02 Kcal/mol) at pH 7.0. Also, only these compound's affinities were found to be reduced at pH 4.5, as evidenced by their lower BE (GC466: -5.06 ± 0.84 Kcal/mol and GC519: -6.75 ± 0.62 Kcal/mol) compared to the others (**Table 3.2**). Similarly, in the analysis of interaction patterns, at pH 7.0 (**Figure 3.3**), rGCase active site residue Trp198 interacted hydrophobically with all ligands (GC466, GC519, GC329, and GC607) but only through stronger conventional H-bonds with GC466 and GC519.

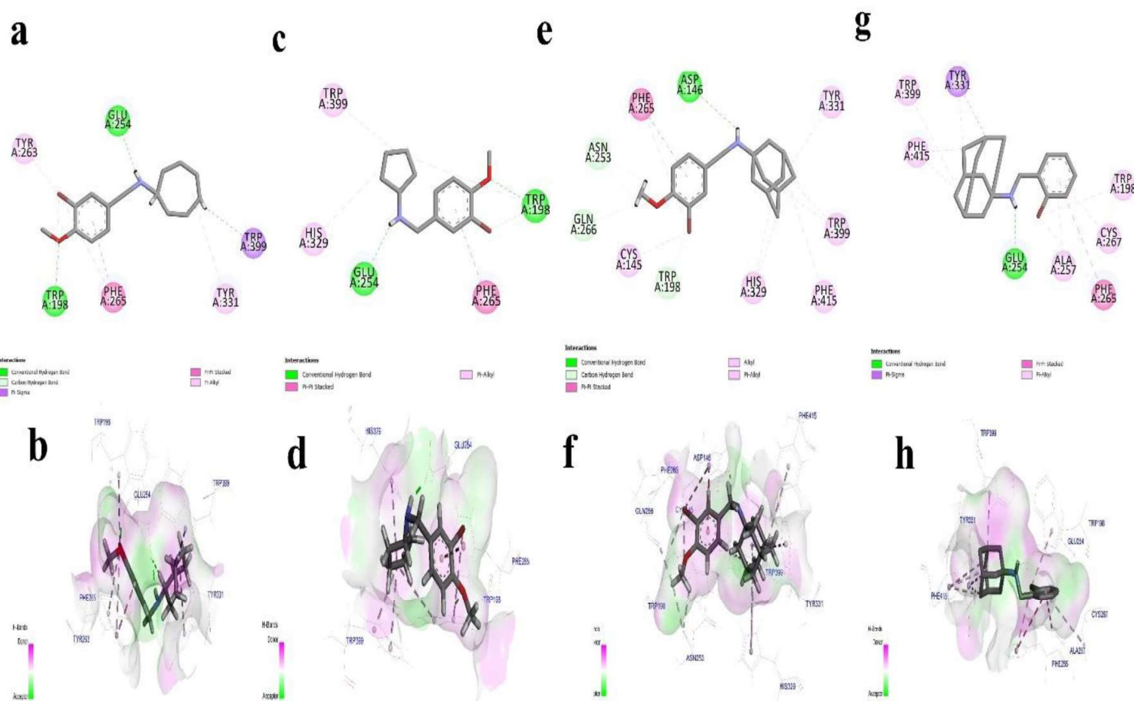

Figure 3.3 2D and 3D interaction of compounds GC466 (a and b), GC519 (c and d), GC329 (e and f), GC607 (g and h) bound with rGCase at pH 7.0.

Glu254, a catalytically active site residue, formed the strongest conventional H-bond with GC466 and GC519 among all ligands. The active site, loop 4 residue Tyr263, interacted only with GC466 (π–alkyl interaction). However, Trp399 interacted *via* π–alkyl with all except GC466. Interestingly, it had a stronger π–sigma interaction with GC466. Furthermore, alkyl, π–alkyl, and carbon-hydrogen (H-C) bonding interactions with GC329 were discovered with residues Cys145, His329 and Phe415, as well as with Asp146, Asn253, and Gln266, respectively. However, GC607 interacted through π–alkyl binding with residues Ala257, Cys267, and Phe415.

At pH 4.5 (**Figure 3.4**), all interactions with the above-mentioned active site residues with compounds GC466 and GC519 were lost, unlike at pH 7.0.

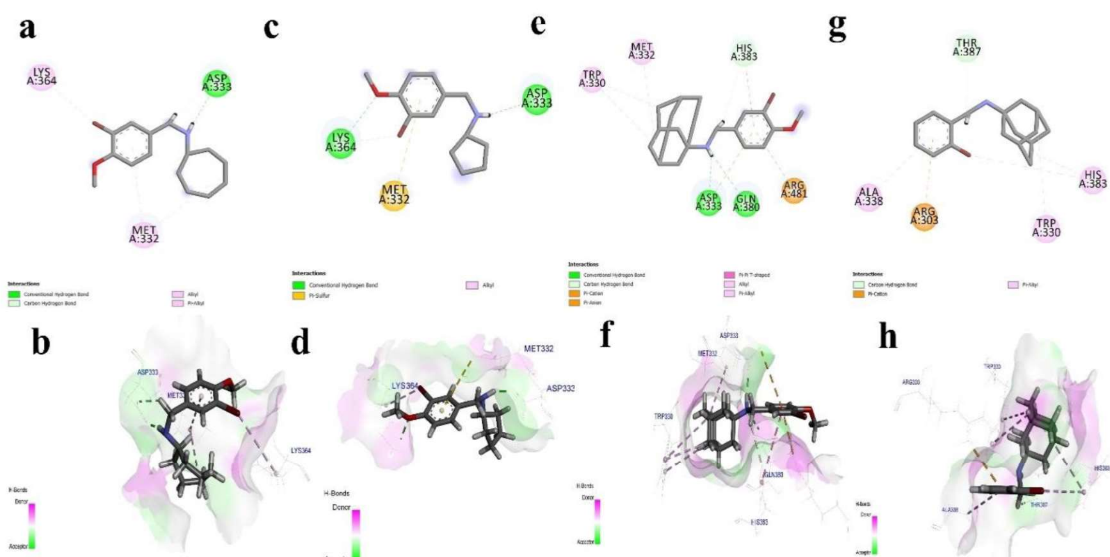

Figure 3.4 2D and 3D interaction of compounds GC466 (a and b), GC519 (c and d), GC329 (e and f), GC607 (g and h) bound with rGCase at pH 4.5.

Albeit, there were a few interactions with GC607 and GC329, but they were with non-active active site residues such as Gln380 (H-bonding), His380 (H-C bonding), and Arg481 (π–cation) with GC329, Arg303 (π–cation), Thr387 (C-H-bonding) and His383 (alkyl) with GC607. The changes occurring in the binding pattern and binding energy at pH 4.5 compared to pH 7.0 were evident in different binding mechanisms. Another possibility, as seen in previous work, could be conformational alterations in the active site at pH 4.5 (Tripathi, Ganeshpurkar et al. 2022).

3.3.3.2 Molecular dynamics (MD) simulation

The stability of protein-ligand complexes at pH 7.0 and 4.5 was investigated using pH-dependent MD simulations. It was evaluated by the root mean square deviation (RMSD), root mean square fluctuation (RMSF), protein-ligand contact time (PL-contact), radius of gyration (R_g), and the solvent accessible surface area (SASA) parameters. Total five MD simulations of rGCase (Apo form), rGCase-GC466, rGCase-519, rGCase-329, and rGCase-GC607 complexes were run for 50 ns.

3.3.3.2.1 RMSD

The average displacement of an atom from an initial position over a trajectory period (50 ns) was calculated using RMSD. If the deviation is smaller, the protein is more stable. At pH 7.0 (**Figure 3.5a**), the average RMSD for rGCase and complexes of rGCase with GC466, GC519, GC329, and GC607 was 1.26 ± 0.15 Å, 1.12 ± 0.09 Å, 1.20 ± 0.06 Å, 1.25 ± 0.11 Å and 1.26 ± 0.14 Å, respectively. Thus, the apo-form displayed a higher deviation than ligand-bound forms. While among them, the lowest deviation was observed for GCase complexed with GC466 and GC519. These findings revealed that both these ligands bind to rGCase and have the good stabilizing capability, as seen by the decreased deviation.

However, at pH 4.5 (**Figure 3.5b**), there were an increase in RMSD was observed for GCase complexed with GC466 (2.02 ± 0.26 Å), GC519 (1.99 ± 0.31 Å), GC329 (1.76 ± 0.16 Å), and GC607 (1.65 ± 0.18 Å) as compared to rGCase apo form (1.43 ± 0.13 Å). The greatest RMSD deviation was seen when ligands GC466 and GC519 were complexed with rGCase, indicating that they had a very low binding affinity and may not be able to accommodate into a cavity at this pH as the simulation progressed.

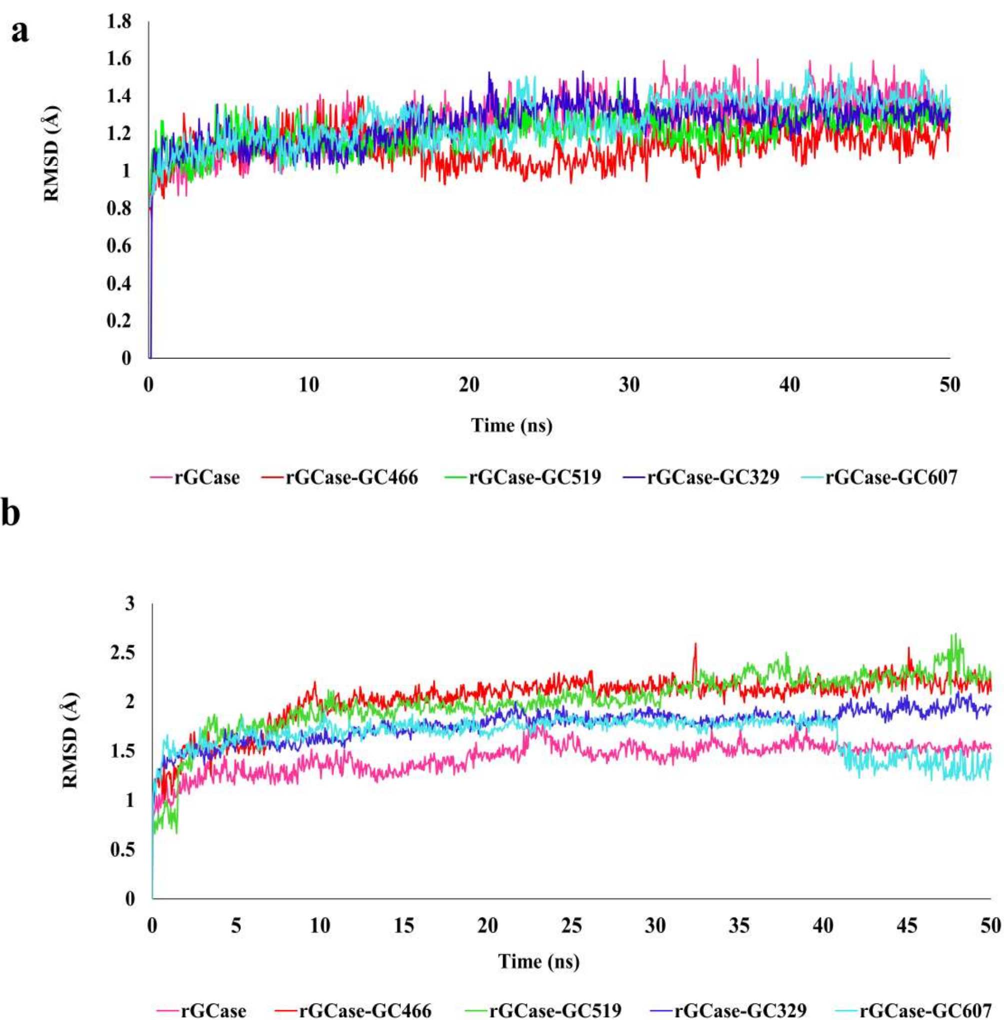

Figure 3.5 Backbone RMSD plots of protein and protein-ligand complexes at pH 7.0 (a) and 4.5 (b).

Similar results were found in ligand RMSD plots, where, among all the ligands (**Figure 3.6a-d**), the deviation of GC466 (7.25 ± 1.54 Å) and GC519 (5.80 ± 0.83 Å) was much higher at pH 4.5 than at pH 7.0 (GC466: 1.42 ± 0.30 Å and GC519: 2.81 ± 0.43 Å), indicating instability of these ligands in acidic conditions. The difference in RMSD values at pH 4.5 could be related to conformational changes in the loops that cap the active site cavity, as demonstrated in our prior study (Smith, Mullin et al. 2017, Nakagome, Kato et

al. 2018, Tripathi, Ganeshpurkar et al. 2022). Poorer ligands-rGCase binding interactions at pH 4.5 compared to pH 7.0 could be another reason, as observed in docking studies.

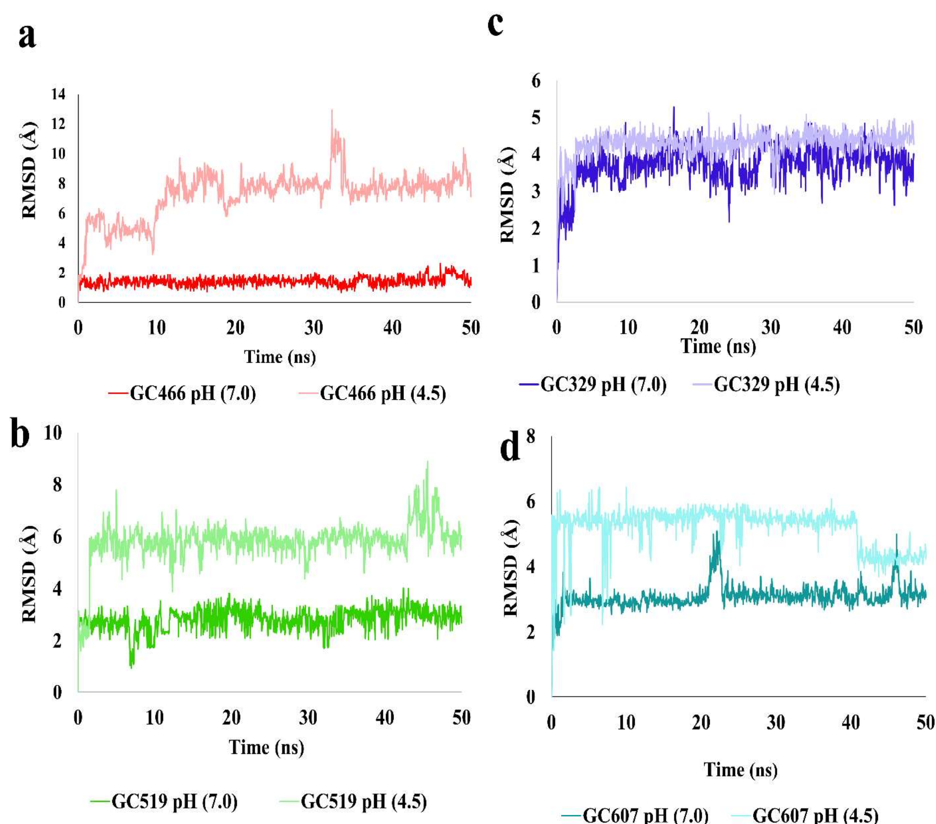

Figure 3.6 RMSD plots of ligands (a-d) at both pHs (7.0 and 4.5).

3.3.3.2.2 RMSF and PL-contacts time

In MD simulation, the RMSF value is used as a measure of overall flexibility. It also examines which particular protein residues interacted with ligands (Hansson, Oostenbrink et al. 2002, Dong, Liao et al. 2018).

The results of RMSF at pH 7.0 (**Figure 3.7a and Figure 3.2 in appendices**) during 50 ns demonstrated that rGCase-GC466 and rGCase-GC519 complexes led to a higher degree of reduction in fluctuations (RMSF values) of the most active site residues like Asp146, Trp198, Asn253, Glu254, Glu358, Trp399, His329–Ala336 (loop 1), Cys360–

Phe365 (loop 2), Asn410–Val416 (loop 3) and Tyr263–Cys267 (loop 4), compared to apo GCase (unbound form). The catalytic residues Glu254 and Glu358 were identified inside the rGCase cavity, surrounded by loops 1–4, and all played a critical role in ligands stabilization. However, compared to rGCase-GC466 and rGCase-GC519, the rGCase-GC329 and rGCase-GC607 complexes had reduced RMSF values with only a few residues (See the residues name in **Figure 3.7a**). Overall, GC466 and GC519 showed stable complexes with rGCase as indicated by the lower RMSF values compared to other ligands. Likewise, in PL-contacts time analysis (**Table 3.2, Figure 3.7b-6c and Figure 3.3 in appendices**), there were revealed that among all ligands, GC466 and GC519 had a higher tendency to maintain interactions with most of the active site residues (names summarized in **Table 3.2**) for more than 30% of simulation time. But, the uttermost interaction was found with GC466 alone, which was 88.4 % with Phe265 and 93.5 % with His329. The strongest H-bonding interaction was noticed for ligand GC466 with residues (Asp146, Trp198, Glu254, Phe265 and Glu358) and GC519 with residues (Asp146, Trp198, Glu254, Tyr263, and Glu358). However, when ligands GC329 and GC607 complexed with rGCase, the number of residues that interacted with them (**Table 3.2**) was lower than GC466 and GC519. These findings showed that at pH 7.0, the interaction of GC466 and GC519 with rGCase was the strongest of all ligands, forming stable complexes.

Table 3.2 PL-contacts time, BE and IC_{50} profiles of compounds for rGCase at pH 7.0 and 4.5.

Compound Code	**pH 7.0**				**pH 4.5**			
	GC466	**GC519**	**GC329**	**GC607**	**GC466**	**GC519**	**GC329**	**GC607**
Active site residues interacted 30% > of simulation times	**9 residues** Asp146 – 68.2% Trp198 – 42% Phe265 – 88.4% Cys267 – 41.6% His329 – 93. 5% Tyr331 – 38.3% Trp399 – 36.2% Phe415 – 32.4% Val416 – 34.8%	**6 residues** Asp146 – 56.4% Tyr263 – 62% Phe265 – 55.4% Tyr331 – 58.3% Glu358 – 60.2% Trp399 – 43%	**4 residues** Trp198 – 54% Phe265 – 64.7% Tyr331 – 51.1% Trp399 – 47.4%	**2 residues** Trp198 – 36.5% Asn253 – 89.6%	*NI.	*NI.	*NI.	*NI.

Active site residues interacted through H-boding	**5 residues** Asp146 – 42% Trp198 – 40.8% Glu254 – 14.4% Phe265-19.7 Glu358 – 17%	**5 residues** Trp198 – 4% Glu253 – 0.5% Glu254 – 3% Tyr263 – 60% Glu358 – 18.4%	**2 residues** Asp146 – 14% Trp198 – 28.5%	1 **residue** Asn153 – 20%	**1 residue** Asp333 – <2.0%	**2 residues** Asp333, Leu335 (Both with <3.0%)	**1 residue** Asp333 – 3.1%	*NI
Non-active site residues interacted 30% > of simulation times	*NI.	*NI.	*NI.	*NI.	*NI.	**2 residues** Arg308 – 36.7% Trp309 – 29.6%	**3 residues** Arg303 – 68.8% Gln80 – 32.4% His383 – 38.6%	**2 residues** His383 – 62.2% Thr387 – 30.4%
Non-active site residues	*NI.	*NI	*NI	*NI	*NI	**2 residues** Arg308 – 18%	**3 residues**	**3 residues**

interacted through H-boding						Trp309 – 15.4%	Arg303 – 16.8% Gln380 – 25.4% His383 – 15.6%	Gln380 – 3.6% His383 – 39.2% Thr387 – 24%
Binding energy (Kcal/mol)	-8.98 ±0.68	-9.66 ±1.02	-8.02 ±0.74	-8.15 ±0.95	-5.06 ±0.84	-6.75±0.62	-7.04±0.76	-7.62±0.86
(IC_{50}, µM)	1.62±0.2	7.03±2.2 [a]	38.74±12.8 [a, b]	34.5±15.3 [a, b]	$NI (1000)	$NI (1000)	@NI (1000)	#NI (500)

All values are of mean ± SD (n=3). [a]p < 0.05 compared to compound GC466 and [b]p < compared to compound GC519. p < 0.05 are considered significant [One-way ANOVA followed by post hoc Tukey test. $NI, non-inhibitory effect (highest concentration measured, µM), @NI, Less than 22 % inhibition at 1000 µM concentration, #NI, Less than 24 % at 500 µM concentration, *NI, not identified.

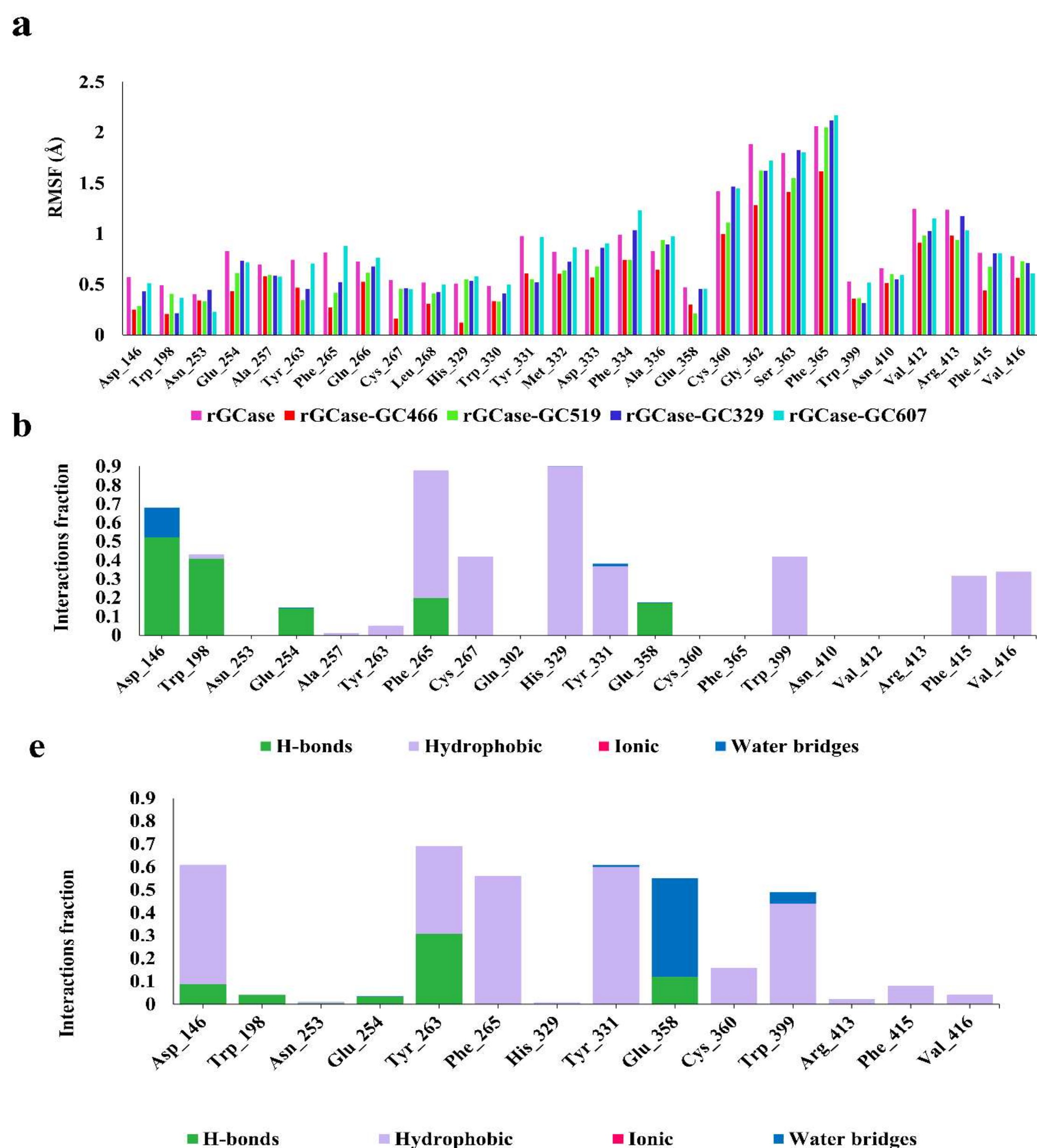

Figure 3.7 Backbone RMSF plots of protein and protein-ligand complexes at pH 7.0 (a). 50 ns PL-contact time frame plots of GC466 (b) and GC519 (c) at pH 7.0. A value of 0.85 indicates that the specific interaction is maintained 85% of the time during the simulation.

At pH 4.5 (**Figure 3.8a and Figure 3.4 in appendices**), it was suggested that no decrease in fluctuations (RMSF) was observed with the aforementioned residues after all four ligands bound, which revealed none of the ligands interacted with rGCase active site residues at pH 4.5; however, they did at pH 7.0.

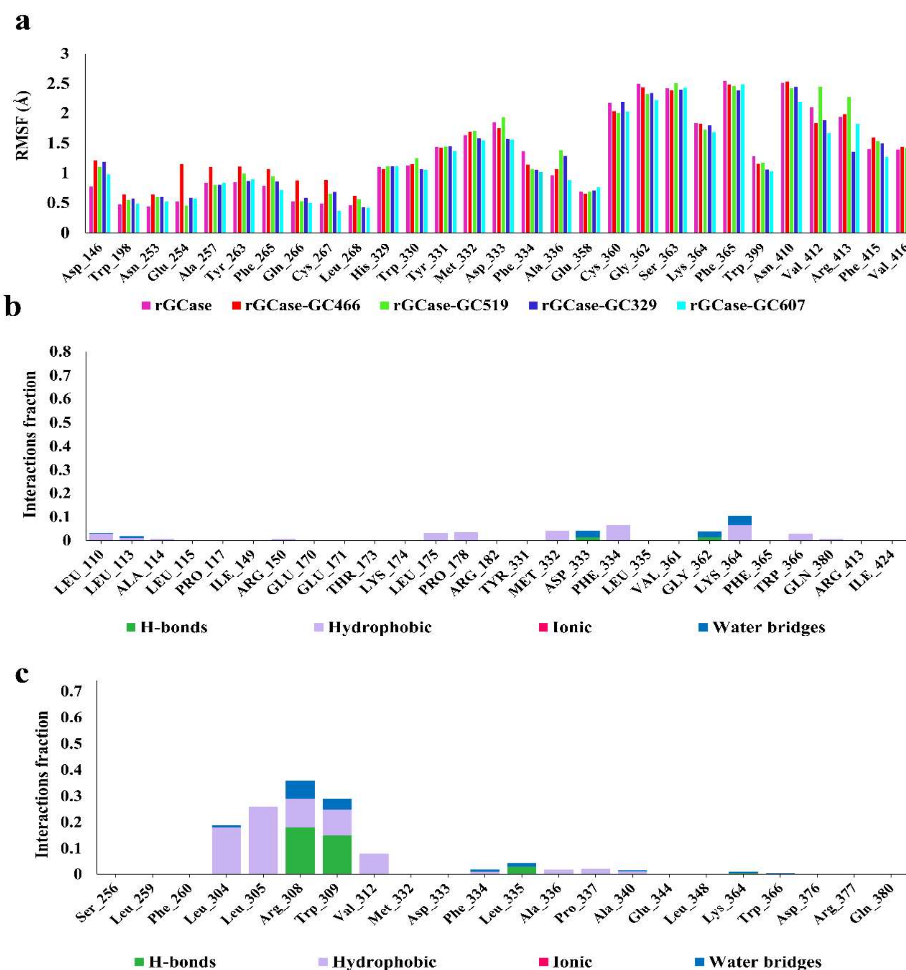

Figure 3.8 Backbone RMSF plots of protein and protein-ligand complexes at pH 7.0 (a). 50 ns PL-contact time frame plots of GC466 (b) and GC519 (c) at pH 4.5. A value of 0.85 indicates that the specific interaction is maintained 85% of the time during the simulation.

The same results were found in the PL-contacts study (**Figure 3.8b -c and Figure 3.5 in appendices**), where none of the ligands interacted much with active site residues, as stipulated by the lowest % of PL-contacts time. The maximum % of the loss was found for GC466 and GC519. These pH-dependency ligands binding with rGCase could be related to conformational changes in the loops near the active site cavity's entry, as shown in a prior study (Smith, Mullin et al. 2017, Nakagome, Kato et al. 2018, Tripathi, Ganeshpurkar et al. 2022).

We next examined the ligands' RMSF (fluctuations) to determine their stability at both pHs. The results showed that all ligands had a higher degree of fluctuations at pH 4.5 (Mean RMSF: 8.49 ± 1.79 Å, 7.45 ± 1.02 Å, 2.69 ± 0.98 Å, and 2.47 ± 0.91 Å for the ligands GC466, GC519, GC329, GC607, respectively) than at pH 7.0 (1.26 ± 0.54 Å, 0.92 ± 0.16 Å, 1.29 ± 0.36 Å, 1.63 ± 0.28 Å for GC466, GC519, GC329, GC607, respectively) across the simulated time (**Figure 3.9a-d and Figure 3.6 in appendices**). These findings showed that all ligands were unstable at pH 4.5, but the instability of GC466 and GC519 was more, as evidenced by the greater RMSF values.

3.3.3.2.3 Measurement of R_g and SASA

The plots of R_g and SASA allow us to evaluate the changes in ligand compactness and solvent accessibility. Higher stability is associated with lower R_g or higher compactness, and *vice versa* (Singh, Ganeshpurkar et al. 2020, Kumar, Seth et al. 2021, Tripathi, Ganeshpurkar et al. 2022). At pH 4.5, ligand's R_g *versus* time plots demonstrated that all ligands had a greater average R_g (4.02 ± 0.20 Å, 3.85 ± 0.14 Å, 4.11 ± 0.12 Å, 3.49 ± 0.15 Å for GC466, GC519, GC329, GC607, respectively) than those at pH 7.0 (1.70 ± 0.13 Å, 2.18 ± 0.15 Å, 3.63 ± 0.73 Å, 3.42 ± 0.66 Å for GC466, GC519, GC329, GC607, respectively) throughout the MD, indicating that they were more compact and stable in the cavity of protein at pH 7.0 than pH 4.5 (**Figure 3.9e-f and Figure 3.7 in Appendices**).

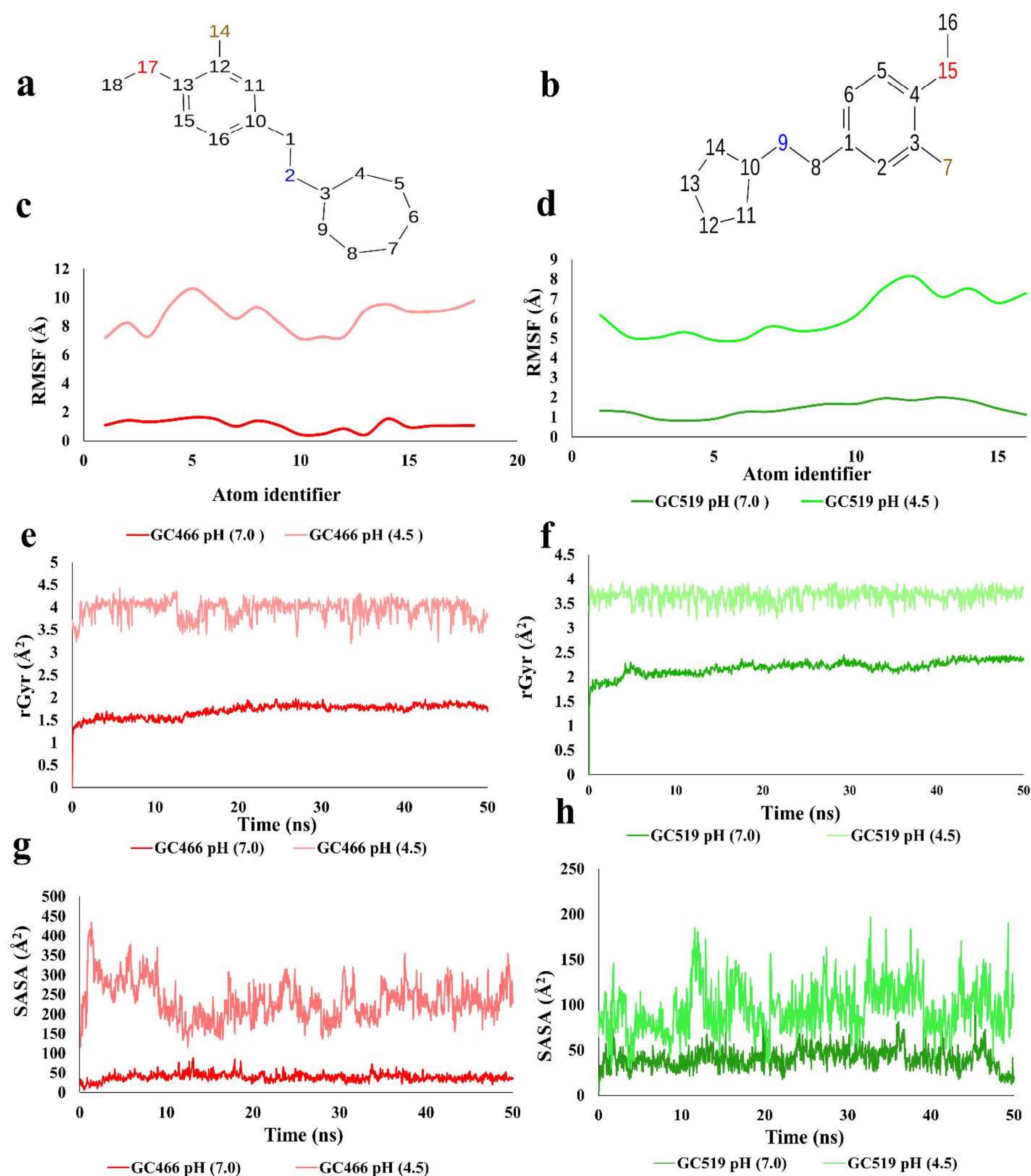

Figure 3.9 Atom identifier of GC466 (a) and GC519 (b). Ligand RMSF plots of GC466 (c) and GC519 (d) at both pHs 7.0 and 4.5. R_g (e and f) and SASA (g and h) plots of ligands at pH 7.0 and 4.5.

Overall, the stability of ligands GC466 and GC519 was higher at pH 7.0 than at pH 4.5 among all ligands. Similar results were obtained when SASA ligands were investigated. We found that at pH 4.5, GC466 and GC519 were unstable, with higher SASA values of 234.15 ± 49.43 and 98.41 ± 23.30, respectively, compared to pH 7.0, which had the lowest SASA values of 20.14 ± 3.69, 29.45 ± 4.8, respectively (**Figure 3.9g-h**). Conclusively, at pH 4.5, the loss of contacts between rGCase active site residues and ligands may result in ligands instability or structural changes in the enzyme, as found in our previous study (Tripathi, Ganeshpurkar et al. 2022). Considering the above findings of the *in silico* studies, we concluded that all ligands showed pH-dependent protein-ligands interactions, but for ligands, GC466 and GC519 were more among them.

3.3.4 *In vitro* pH-dependent enzyme study

3.3.4.1 Estimation of IC_{50}

As we scrutinized in our above study, the ligand-interaction strength was greater at ER pH (7.0) than at lysosomal pH (4.5). As a result, here we chose these two pHs to assess the compounds' pH-dependent effect on rGCase activity. At pH 7.0, GC466 and GC519 were the most effective test compounds, requiring 23.8-fold and 21.2-fold less concentration (IC_{50}) than GC329 and GC607, respectively. In contrast, GC519 required 5.5-fold and 4.9-fold less IC_{50} than GC329 and GC607, respectively, to achieve a similar effect on enzyme inhibitory activity (**IC_{50} values are summarized in Table 3.2**). Also, GC466 and GC519 were the only two highly pH-dependent compounds among the four that showed no inhibition of enzyme activity (IC_{50} not found) when the pH was shifted from 7.0 to 4.5. However, an inhibition in enzyme activity was noticed by compounds GC329 and GC607 at pH 4.5 but at a higher concentration (**Table 3.2 and Figure 3.8 in**

appendices). In summary, the compounds' IC_{50} decreased as pHs decreased, which is consistent with our above *in silico* study, where we found that the compounds' binding interactions for rGCase decreased as pHs decreased. The decrease in IC_{50} at pH 4.5 could be due to the ligand instability or loss of interactions and contact times between ligands and rGCase active site residues, as shown in MD simulation studies. Conformational changes in the active site loops, as seen in our previous study, could also be a factor (Tripathi, Ganeshpurkar et al. 2022).

3.3.4.2 Evaluation of test compounds chaperoning property

The ability of target compounds to behave as pharmacological chaperones were assessed by their ability to stabilize enzymes under thermal denaturation conditions (Trapero, Gonzalez-Bulnes et al. 2012). In this context, the thermal denaturation assay (TDA) method was used where the enzyme was denatured thermally at various functions of time in the presence or absence of a different concentration of test compounds (**Concentration mentioned in Table 3 and Figure 3.9 in appendices**). The chaperoning characteristic was measured in terms of SR. The top three compounds (GC466, GC519, and GC329) were chosen for this study. **Table 3.3** summarizes the stabilization ratio values found for each compound at varying concentrations and incubation periods.

Table 3.3 Time and concentration-dependent stabilization ratios of compounds after thermal denaturation (48 ^{0}C).

Compound code	Concentrations (µM)	Stabilization ratios		
		20 min	**40 min**	**60min**
GC466	2.5	1.52	1.77	2.88
	5	2.07	$4.11^{a,x}$	$6.05^{a,x}$
	10	2.42	$4.83^{a, x}$	$10.20^{a,b,x,y}$
GC519	15	1.52	1.83	2.55
	30	1.94	2.72	$4.54^{\#,x,y}$
	60	2.21	3.72	$6.18^{\#,x,y}$
GC329	50	1.36	1.22	1.33
	100	1.68	1.14	1.54
	150	2.00	1.61	1.63

$^{a}p < 0.05$ compared to 2.5 µM of GC466, $^{b}p <$ compared to 5 µM of GC466, $^{\#}p <$ compared to 15 µM of GC519, $^{x}p <$ compared to 20 minutes, $^{y}p <$ compared to 40 minutes. $p < 0.05$ are considered significant [Two-way ANOVA followed by Bonferroni multiple comparison test.

GC466 was one of three compounds with potential chaperoning properties that significantly stabilized the rGCase in a time and concentration-dependent manner. The maximum SR of GC466 was found after 1 hour of heating at 48 °C, with a SR of 10.20 only at 10 µM. However, GC519 and GC329 were clearly less potent than GC466, requiring 6-fold (60 µM) and 15-fold (150 µM) higher concentrations than GC466, and stabilizing rGCase with SR of 6.18 and 1.63, respectively. Compounds' ability to stabilize rGCase activity could be attributed to the fact that they bound and stabilized rGCase prior to denaturation. The ability of compounds to bind to rGCase in order to stabilize it reflects

their chaperoning ability. Our above *in silico* studies implied this result, demonstrating that test compounds stabilize the rGCase protein by interacting with its active site residues.

3.3.4.3 Binding mode Study

The ideal chaperones have reversible inhibitory natures; thus, a binding mode study is one of the key parameters for testing compounds' reversibility to test them for ideal chaperones. An earlier protocol was used with minor modifications to determine the reversible inhibition of the

enzyme by the most active compounds (GC466 and GC519). In this study, we chose the pH of ER (7.0) because only compounds bind the enzyme at this pH, as discovered in the previous study (Trapero, Gonzalez-Bulnes et al. 2012, Tripathi, Ganeshpurkar et al. 2022). According to the findings, both tested compounds act as reversible inhibitors of the rGCase enzyme. Following treatment with each compound at the concentrations of 10 × IC_{50} and 100 × IC_{50}, the activity of rGCase was reduced to a minimum (see **Figure 3.10**). However, after 100-fold dilution with substrate solution, compounds GC466 (**Figure 3.10a**) and GC519 (**Figure 3.10b**) recovered this activity to 90 - 95 % of control for 0.1 × IC_{50} dilution and 50 - 70 % of control for 1 × IC_{50} dilution. Previous research has also shown that the compounds follow a reversible series if the enzyme recovers more than 90% and 50% of its activity after diluting the enzyme-inhibitor mixtures to 0.1 × IC_{50} and 1 × IC_{50}, respectively (Minders, Petzer et al. 2015, Kumar, Dwivedi et al. 2018).

3.3.4.4 Enzyme kinetics

A kinetics study with the most potent compounds (GC466 and GC519) was performed to determine the mechanism of inhibition of rGCase by exploring the enzyme kinetics parameters such as V_{max} and K_m. The pH of 7.0 was selected for this experiment because compounds bind to enzymes only at this pH. The V_{max} and K_m were calculated by plotting

the Michaelis-Menten curves (**Figure 3.10c and f**) between velocities and substrate concentrations. Obtained findings revealed that V_{max} and V_{max}/K_m (slope) in the Michaelis-Menten graph decreased as inhibitor concentration increased, while K_m (intercept) increased (**Figure 3.10d and g**). These V_{max} and K_m patterns indicated that both compounds exhibited a mixed-type inhibition model at the ER pH 7.0, acting on free enzymes and enzyme-substrate complexes. Meanwhile, we used a Dixon plot to calculate the compounds' binding affinity at the same pH in terms of K_i (inhibition constant) (replots the slopes of reciprocal velocity versus inhibitor concentrations, see **Figure 3.10e and h**). The lower the inhibitor's affinity for the enzyme, the greater the K_i value. Compound GC466 inhibited the rGCase with a K_i value of 0.64 ± 0.2 μM (**Figure 3.10e**) at pH 7.0. However, compound GC519 increased the K_i value by 6.5-fold (4.17 ± 3.4 μM, **Figure 3.10h**) compared to GC466, indicating that GC466 had a higher binding affinity at the ER pH 7.0 than compound GC519. Loss in protein-ligand contact time with rGCase active site residues Trp198, Glu254, Phe265, Cys267, His329, Tyr331, Phe415, and Val416 by GC519 as compared to GC466 could also be a reason for losing affinity of GC519, compared to GC466. Another possible explanation is that GC519 is more unstable than GC466 at pH 7.0, as seen in MD in the study.

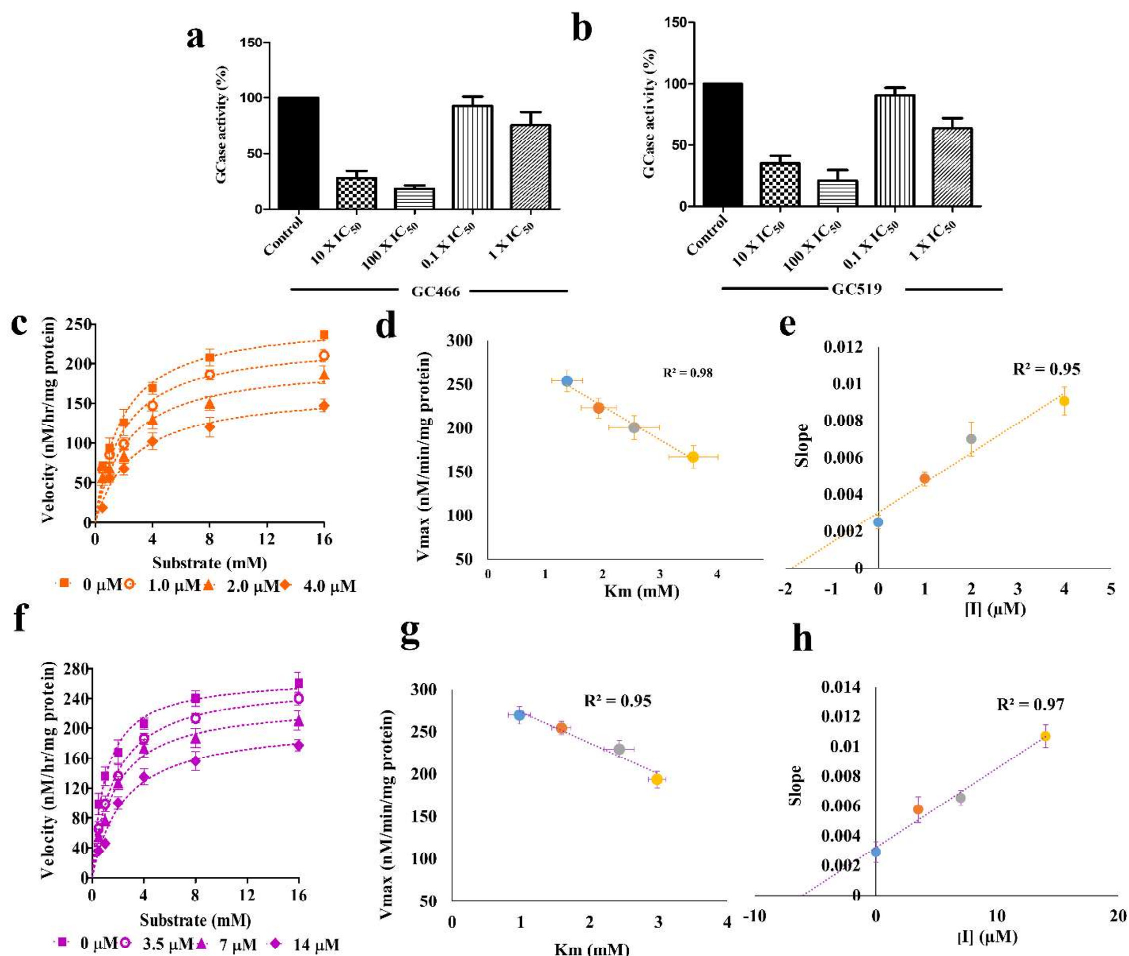

Figure 3.10 a (GC466) and b (GC519) show compounds' reversibility study at pH 7.0. Michaelis Menten curves (c and f), K_m *versus* V_{max} plots (d and g), and Dixon plots (e and h) of GC466 (red) and GC519 (green) at pH 7.0. All values are mean ± SD [Non-linear regression analysis, Graph Pad Prism 5.1 Software, Inc.].

3.3.5 Cell line study

3.3.5.1 Neurotoxicity assay

The MTT assay method was used to investigate the effect of the most potent compounds (GC466 and GC519) on neurotoxicity in terms of cell viability. Exposing the cells to

various concentrations of each compound alone had no significant effect [F (6, 20) = 1.15; p < 0.05,

Figure 3.11a, F (6, 20) = 2.49; p < 0.05, **Figure 3.11b**, one way ANOVA method] on cell viability or neurotoxicity in SH-SY5Y cells as compared to control until 75 μM. Thus, these test compound ranges are safer for further studies.

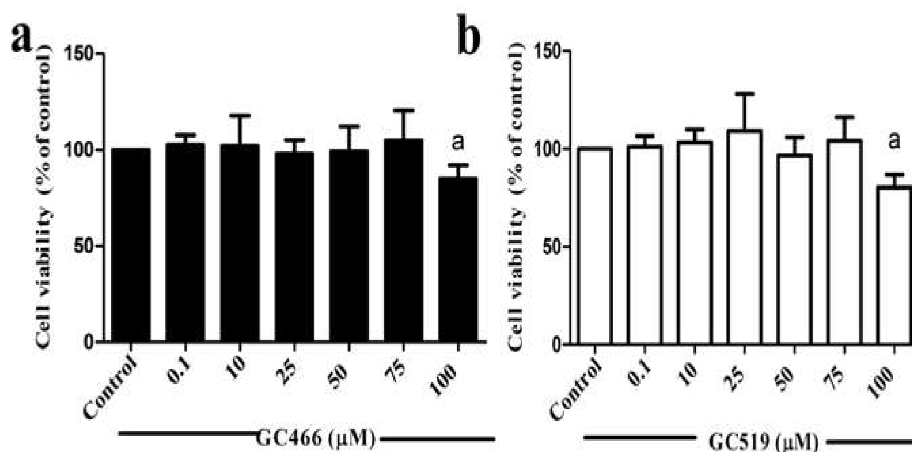

Figure 3.11 Neurotoxicity study of the test compound GC466 (a) and GC519 (b) on neuroblastoma SH-SY5Y cell line. All values as in the form of mean ± SD (n=3). [a] p < 0.05 compared to control [One or Two-way ANOVA followed by Tukey tests, Graph Pad Prism 5.1 Software, Inc.].

3.3.5.2 Evaluation of test compounds on 6-OHDA-induced cell line model

3.3.5.2.1 Neurorestorative activity assay

In the first set of experiments, we investigated the concentration and incubation time of 6-OHDA to develop a neurotoxicity model of PD. Two-way ANOVA analysis revealed significant differences in cell viability among groups [F (1, 40) = 1.92; p < 0.05], time [F (9, 40) = 20.96; p < 0.05] and interaction between group and time [F (9, 40) = 138.3; p <

0.05] as depicted in **Figure 3.12**. Based on our findings, 6-OHDA significantly reduced cell viability in a dose and time-dependent manner. After 6 hours of exposure to 6-OHDA at 150 µM concentration, cell viability was reduced by 76.4 ± 9.4 % (control, 100% cell viability). Several studies have concluded that cell viability loss of more than 65 % is a valid 6-OHDA-induced neurotoxicity model for PD (Guo, Bezard et al. 2005, Luo, Wei et al. 2012, Li, Liu et al. 2020), so we used these concentrations to generate the cell line model of PD in subsequent studies.

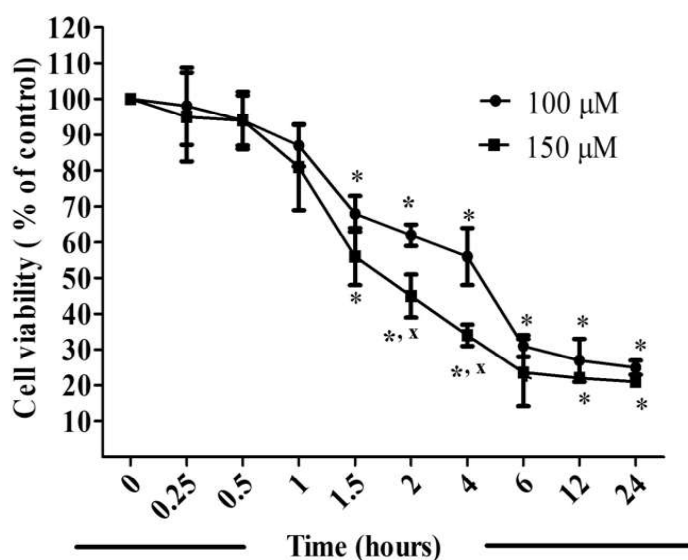

Figure 3.12 6-OHDA-induced changes in cell viability at the indicated concentrations and time points. All values as in the form of mean ± SD (n=3). $^{*}p < 0.05$ compared to control (0 µM 6-OHDA), $^{x}p < 0.05$ compared to the corresponding time of 100 µM of 6-OHDA [Two-way ANOVA followed by Bonferroni multiple comparison tests, respectively, Graph Pad Prism 5.1 Software, Inc.].

As we know, the symptoms of PD appear only after about 70-80% of the cell death, and there is no proven therapy to restore sick neurons ('neurorestorative') to a normal state

(Dawson and Dawson 2002). Thus, in the second set of experiments, we evaluated the neurorestorative effect of test compounds against the cell line model of PD. For comparison, selegiline (a well-known anti-PD drug) and AMB (first GCase-acting drug to be tested as a disease-modifying therapy for PD) were used as standard drugs. The one-way ANOVA results revealed that cell viability differed significantly [[$F (9, 29) = 22.62$; $p < 0.05$, **Figure 3.13**] among groups. After 6 hours of exposure, 6-OHDA caused a significant reduction in cell viability, with the remaining activity being 23.8 ± 7.33% compared to the control (100 % cell viability). However, cells treated with GC466 (5 µM) for 48 hr after 6 hr exposure to 6-OHDA were more effective, significantly restoring cell viability to 71.6 ± 19.2% compared to the control. This neurorestorative effect by the GC466 was concentration-dependent (between 1.25 and 5 µM) in this PD cell line model. In comparison, AMB and SEL required 5 and 2-fold more concentrations but restored to only 63.5 ± 9.8% and 46.2 ± 5.3% cell viability, respectively.

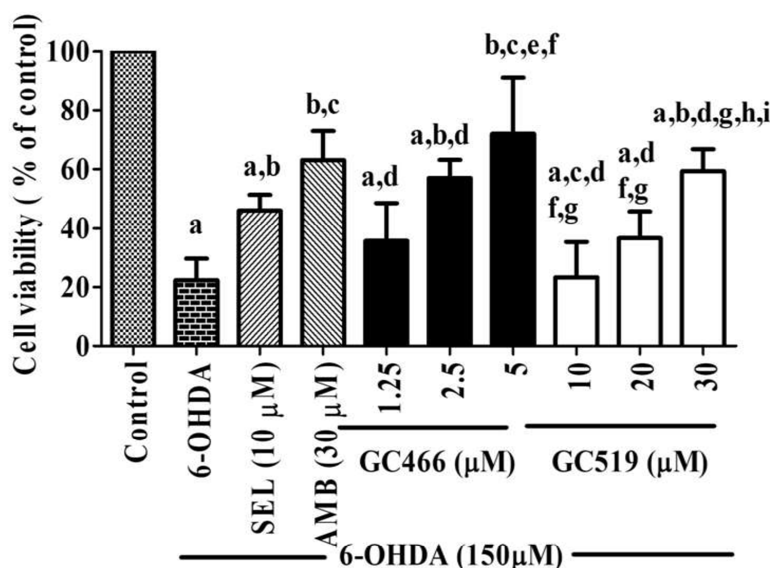

Figure 3.13 Neurorestorative effects of test compounds against the 6-OHDA-induced PD cell line model. All values as in the form of mean ± SD (n=3). $^{a}p < 0.05$ compared to control, $^{b}p < 0.05$ compared to 6-OHDA, $^{c}p < 0.05$ compared to 6-OHDA + SEL, $^{d}p < 0.05$ compared to 6-OHDA + AMB, $^{e}p < 0.05$ compared to 6-OHDA + 1.25 μM, $^{f}p < 0.05$ compared to 6-OHDA + 2.5 μM, $^{g}p < 0.05$ compared to 6-OHDA + 5 μM, $^{h}p < 0.05$ compared to 6-OHDA + 10 μM, $^{i}p < 0.05$ compared to 6-OHDA + 20 μM [One - way ANOVA followed by Tukey tests, respectively, Graph Pad Prism 5.1 Software, Inc.].

3.3.5.2.2 GCase activity assay

GCase enzyme dysfunction in PD patients makes GCase a significant risk factor for the disease (Do, McKinney et al. 2019). As a result, we assessed the effect of the test compounds on GCase activity. The level of GCase was found to be significantly [$F_{(9, 29)} = 12.42$; $p < 0.05$, **Figure 3.14**] different between groups when analyzed using one-way ANOVA.

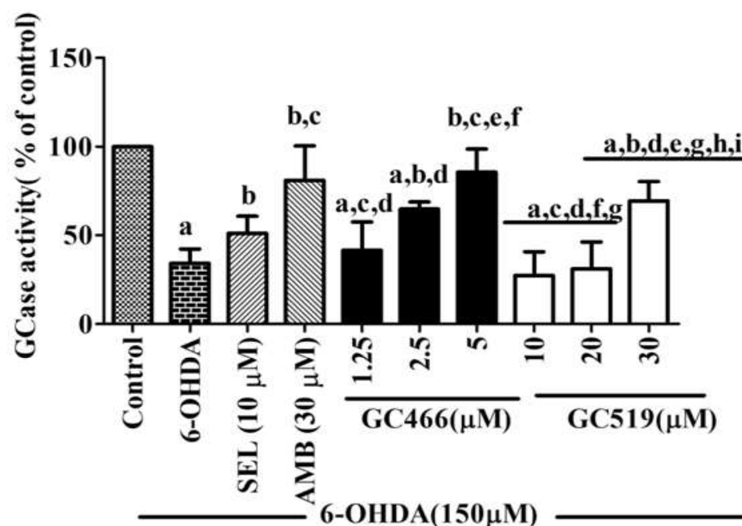

Figure 3.14 Glucocerebrosidase activity assay of test compounds against the 6-OHDA-induced PD cell line model. All values as in the form of mean ± SD (n=3). [a] $p < 0.05$ compared to control, [b]$p < 0.05$ compared to 6-OHDA, [c]$p < 0.05$ compared to 6-OHDA + SEL, [d]$p < 0.05$ compared to 6-OHDA + AMB, [e]$p < 0.05$ compared to 6-OHDA + 1.25 μM, [f]$p < 0.05$ compared to 6-OHDA + 2.5 μM, [g]$p < 0.05$ compared to 6-OHDA + 5 μM, [h]$p < 0.05$ compared to 6-OHDA + 10 μM, [i]$p < 0.05$ compared to 6-OHDA + 20 μM [One - way ANOVA followed by Tukey tests, respectively, Graph Pad Prism 5.1 Software, Inc.].

6-OHDA exposure in SH-SY5Y cells for 6 hr reduced GCase activity by 65.83 ± 8.03%, compared to control. Treatment with GC466 (5 μM) and GC519 (30 μM) restored GCase activity by 48 % and 35 %, respectively, after 6 hr of 6-OHDA exposure for 48 hr, reaching a maximum of 82.4 ± 13.9% and 62.7 ± 11.3%, respectively. SEL and AMB were less potent than GC466, requiring a 2 to 6-fold higher concentration but only restoring 46.6 ± 9.4% and 78.4 ± 14.8 % of GCase activity, respectively.

3.3.5.2.3 Measurement of Reactive oxygen species (ROS) level

In order to measure whether the increase in ROS level is involved in 6-OHDA-induced cell death and GCase dysfunction, the cells were treated with given concentrations, as shown in **Figure 3.15** The most potent compound, GC466, was chosen for this study.

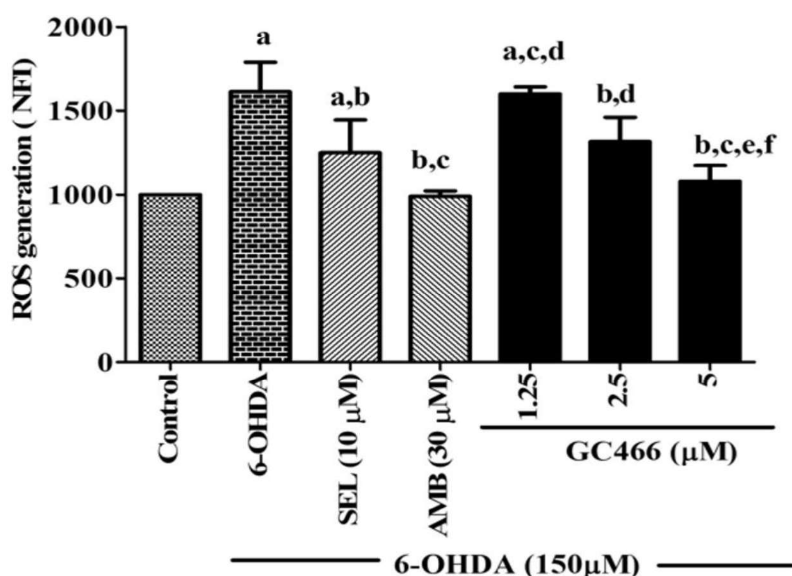

Figure 3.15 Reactive oxygen scavenging activity of test compounds against the 6-OHDA-induced PD cell line model. All values as in the form of mean ± SD (n=3). $^{a}p < 0.05$ compared to control, $^{b}p < 0.05$ compared to 6-OHDA, $^{c}p < 0.05$ compared to 6-OHDA + SEL, $^{d}p < 0.05$ compared to 6-OHDA + AMB, $^{e}p < 0.05$ compared to 6-OHDA + 1.25 µM, $^{f}p < 0.05$ compared to 6-OHDA + 2.5 µM, $^{g}p < 0.05$ compared to 6-OHDA + 5 µM, $^{h}p < 0.05$ compared to 6-OHDA + 10 µM, $^{i}p < 0.05$ compared to 6-OHDA + 20 µM [One - way ANOVA followed by Tukey tests, respectively, Graph Pad Prism 5.1 Software, Inc.].

The one-way ANOVA analysis revealed a significant [$F (6, 20) = 13.6$; $p < 0.05$] difference in ROS levels between groups. 6-OHDA exposure increased ROS levels by 63.2 ± 10.4% compared to the control. However, compared to the control group, the GC466-treated group scavenged ROS in a dose-dependent manner, with 5 µM being more effective against 6-OHDA-induced cell death. It required 2 and 6 times less concentration than SEL and AMB, respectively, to scavenge the ROS; thus, it was a more potent compound among others. Based on cell line research, we can conclude that the compounds' neurorestorative effect on SH-SY5Y cells may be due to scavenging ROS and restoring GCase activity.

3.3.6 Measurement of protein-ligand interaction stability

CD, FT-IR, and Raman spectroscopies were used to confirm the MD findings about the stability of protein-ligand interactions and pH-dependent conformational changes in rGCase. At pH 7.0, the rGCase CD profile revealed α-helix band, along with two negative bands around 209 and 222 (**Figure 3.16a-b and Page 228 – 230 in Appendices**) (Xu, Han et al. 2011, Zhang and Ma 2013, Ding, Yu et al. 2022). Its content was 18.40 ± 0.15%; however, when the pH was changed to 4.5, this % fell to 15.42 ± 0.13%, demonstrating changes in the rGCase structure at pH 4.5. Similar findings were observed using FT-IR [**Page 231- 232 and Figure 3.10 in appendices**] and Raman spectroscopy [**Figure 3.16c-d and Page 233 – 234 in Appendices**], which revealed a shift in the amide I band in the α-helix region (1650–1660 cm–1) as the pH changed from 7.0 to 4.5. Similar observation (changes in α-helix) we noticed in our aforementioned (**Figure 3.1 in appendices**) and previous *in silico* study when comparing these two pHs, changes in the

position of hydrogen bond formation could be the reason for it, as previously described (Zhang and Ma 2013, Ding, Yu et al. 2022, Tripathi, Ganeshpurkar et al. 2022). Meanwhile, rGCase-GC466 interaction and its stability were also investigated at pH 7.0 and 4.5. Spectroscopic findings demonstrated that GC466 stability interacted with the C=O group of protein subunits only at pH 7.0, as indicated by a shift in the position of the amide I peak when compared to it with the same pH of free rGCase (**spectral details are on Pages 228–234 in appendices**). To analyse further, the rGCase-GC466 stability was again measured under thermal denaturation conditions at pH 7.0. At this pH, we found that GC466 bound to the C=O subunit of the rGCase protein and stabilized it before it became denatured.

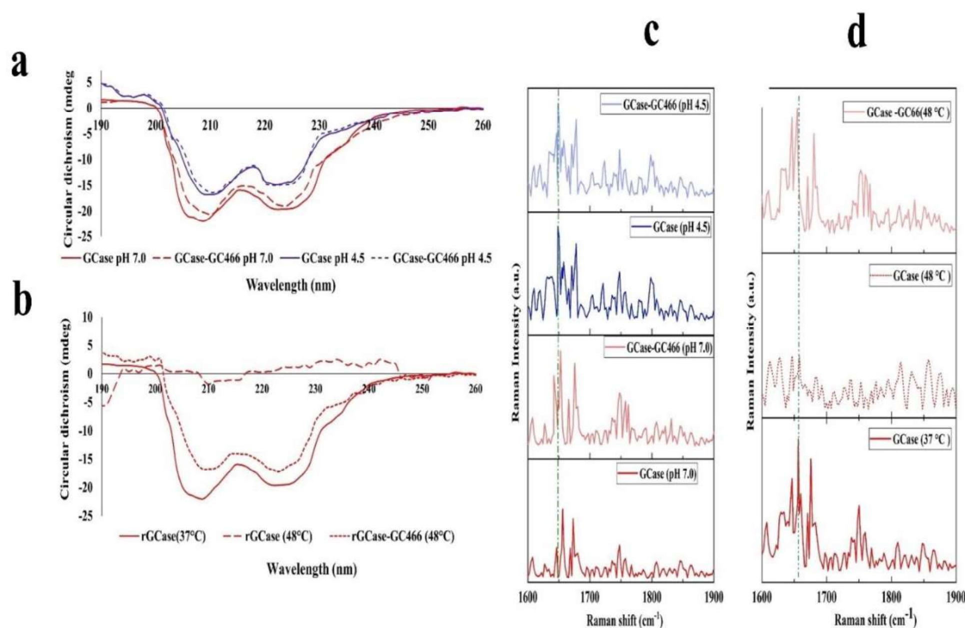

Figure 3.16 Circular dichroism (a) and Raman (c) spectra of the free rGCase protein in either presence or absence of GC466 at pH 7.0 and 4.5. CD (b) and Raman spectra (d) of rGCase protein under thermal denaturation (48 ^{0}C) condition in either presence or absence of GC466 at pH 7.0. rGCase protein kept at 37 ^{0}C (body temperature) is considered as control GCase. The dotted green straight line indicates the Raman shift of rGCase protein.

The ability of compounds to bind to rGCase in order to stabilize it reflects their chaperoning ability. This research was backed with our findings from the MD simulation and *in vitro* study, where we found that GC466 stably interacted with rGCase and inhibited it only at pH 7.0, respectively. However, a detail of the spectroscopic findings has been provided in an appendices file [**Page 228 - 234 in Appendices**].

3.4 Conclusion

Novel glucocerebrosidase chaperones with potential GCase stabilizing action were identified. *In silico* virtual screening, molecular docking, molecular dynamics, and extensive *in vitro* studies have been done to identify appropriate chaperons with stronger protein stabilizing capacity. From the *in silico* and associated analyses, we were able to select four compounds (GC466, GC519, GC329, and GC607) with appropriate BBB penetration, drug-likeness properties, and GCase stabilization abilities. Only one of them, GC466, has been shown by *in vitro* TDA and enzyme kinetics assay to have better chaperoning ability and binding affinity towards GCase compared with others. It required 6-fold (60 µM) and 15-fold (150 µM) less concentration than those of GC519 and GC329 to stabilize the GCase under *in vitro* TDA, respectively. Similarly, GC466's binding affinity (K_i) for GCase was 6.5 times stronger and required just 0.64 ± 0.2 µM to stabilize the enzyme, compared to the second most active compound GC519 (4.17 ± 3.4 µM) evaluated in the *in vitro* enzyme kinetic assay. MD modeling accurately anticipated this GCase-GC466 complex stability and was further verified by *in vitro* CD, FT-IR, and Raman studies. GC466 was also found to have neuroprotective action, GCase potentiating activity, and ROS scavenging capabilities in the cell line investigation. Thus, GC466 being the potential GCase chaperone, may be further developed as a disease modifying agent for PD therapy. However, further pharmacokinetic profiles and *in-vivo* mechanistic

studies on the PD model (with its additional markers) should be explored to confirm its exact role within the PD treatment pipeline.

3.5 Summary

- GC466 was identified as the ideal rGCase chaperone, which binds rGCase with greater affinity at pH 7.0 than at pH 4.5.
- TDA confirmed GC466's chaperoning action by stabilising rGCase before denaturation.

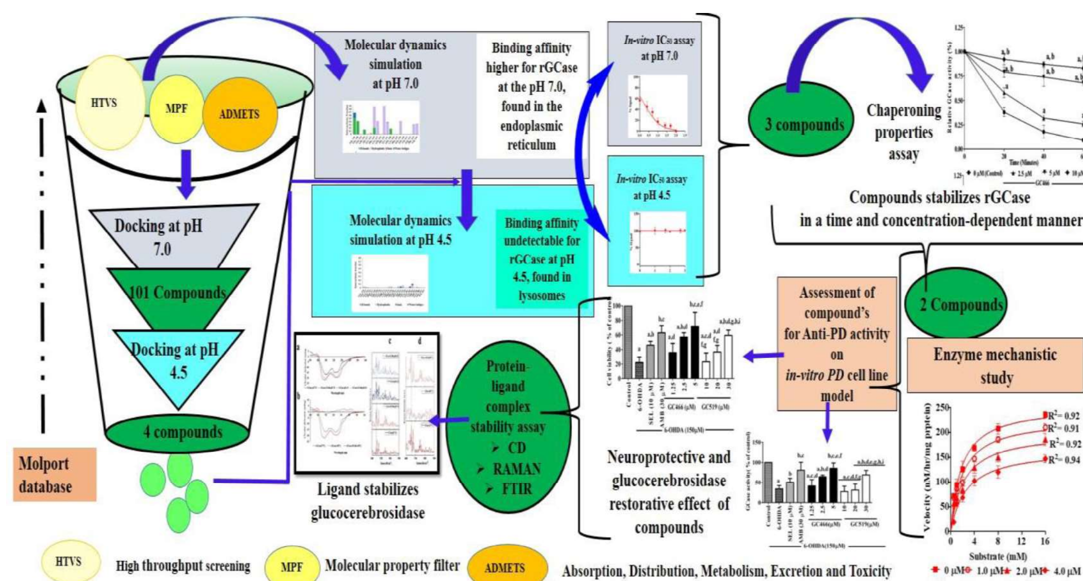

Figure 3.17 elegantly depicts the conclusive findings derived from the meticulous screening and evaluation process of various compounds for the GCase chaperoning assay.

- Asp146, Phe265, His329, and Tyr331 residues play a vital role in the GC466-rGCase complex stabilization.
- *In vitro* pH-dependent CD, FT-IR, and Raman spectroscopies confirmed *in silico* pH-dependent protein-ligand stabilization.
- GC466 shows anti-PD activity in SHSY-5Y cell lines because it enhanced GCase and ROS scavenging activities.